EFFECT OF RADIUS OF CURVATURE OF COATING DIE CORNERS ON THE PINNING OF STATIC CONTACT LINE

Oldrich Joel Romero
Department of Mechanical Engineering Pontificia Universidade Catolica do Rio de Janeiro. Rio de Janeiro, RJ, 22453-900, Brazil.
oldrich@mec.puc-rio.br

L. E. Scriven
Department of Chemical Engineering and Materials Science, University of Minnesota, MN, USA.
pjensen@cems.umn.edu

Márcio da Silveira Carvalho
Department of Mechanical Engineering Pontificia Universidade Catolica do Rio de Janeiro. Rio de Janeiro, RJ, 22453-900, Brazil.
msc@mec.puc-rio.br

Abstract. *Corners are not mathematical. Contact lines do not actually pin. The effects of rounding the downstream corner slot dies on contact line location, effective contact angle, and low-flow limit –air-fingers penetrating from downstream and breaking apart the coating-bead– are examined by solving the Navier-Stokes system for Newtonian flow. The geometry of the die surface is represented by two straight lines and an arc of circle connecting them. The local contact angle is treated as a specified equilibrium value. The system of equation is solved by Galerkin's method and finite element basis functions. The results show how the corner rounding affects the contact line position and stability of the flow, and indicate the minimum radius of curvature necessary to apparently pin the contact line.*

Keywords: *contact line, slot coating, low-flow limit, die corner.*

1. Introduction

Slot coating is commonly used in the manufacturing of adhesive and magnetic tapes, specialty papers, imaging films, and many other products. In this process, the coating liquid is pumped to a coating die. Exiting the slot, the liquid fills the gap between the adjacent die lips and the substrate translating rapidly past them. The liquid in the gap, bounded upstream and downstream by gas-liquid interfaces, or menisci, forms the coating bead, as shown in Fig. 1. In order to sustain the coating bead at higher substrate speeds a slight vacuum is applied to the upstream meniscus [Beguin (1954)]. The thickness of the coated liquid layer is set by the flow rate fed to the coating die and the speed of the moving substrate, and is independent of other process variables is ideal for high precision coating. However, the nature of the flow in the coating bead and the uniformity of the liquid layer it delivers can be affected by the substrate speed, liquid properties, configuration of the die lips and cross-web uniformity of the contact lines position.

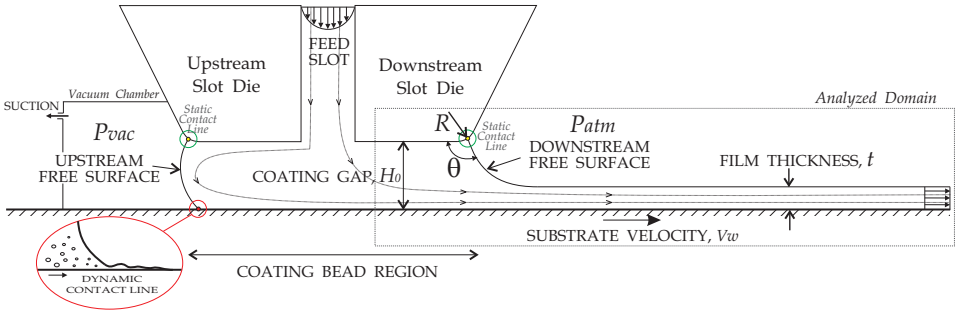

Figure 1. Sketch of slot coating process.

[Romero *et al.* (2004)] reviews the different analysis of slot coating flows and predictions of the coating window of the process for both Newtonian and non-Newtonian liquids. For low viscosity liquids, the most important limit in slot coating process occurs when, at a given substrate speed, too low flow rate per unit width from the slot causes the downstream meniscus to curve so much that it cannot bridge the gap's clearance H_0. Consequently the meniscus becomes progressively more three-dimensional, alternate parts of it invading the gap until the bead takes a form that delivers separate rivulets to the substrate moving past, as illustrated in Fig. 2. This transition from a continuous coated liquid layer is what is called here the *low-flow limit*: the minimum thickness of liquid that can be deposited from a gap of specified clearance at a given substrate speed. It is independent of the vacuum applied, given that the vacuum is great enough to draw the upstream

meniscus away from the feed slot.

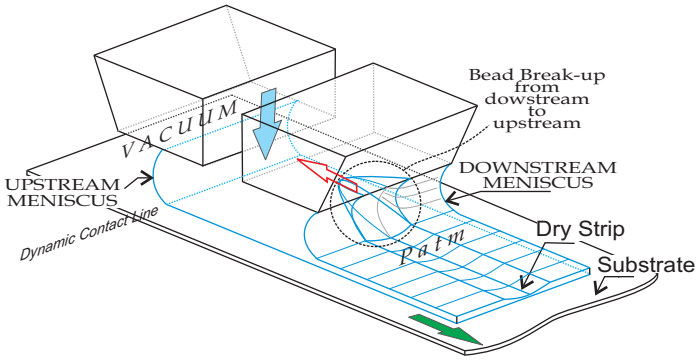

Figure 2. Three-dimensional sketch of the bead break-up from the upstream meniscus, which marks the onset of the low-flow limit in slot coating process.

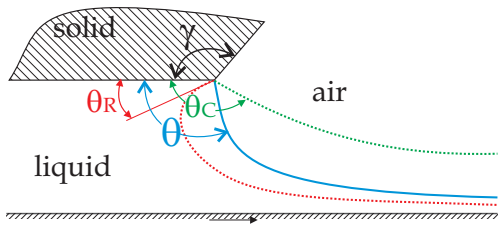

Figure 3. Geometrical representation of the Gibbs' condition $\theta_R < \theta < \theta_C$, where $\theta_C = \theta_A + 180^o - \gamma$.

The theoretically determined low-flow limit was defined by [Carvalho and Kheshgi (2000)], [Romero *et al.* (2004)] and [Romero *et al.* (2005)], as the flow rate at which the static contact angle θ between the downstream free surface and the downstream die lip became less than 10^o. Their analysis assumed that the downstream free surface was pinned at the corner between the downstream die lip and shoulder. This is a simplified view of the problem, because corners are not mathematical and contact lines do not actually pin.

In practice, it is important that the location of the contact line is uniform in the transverse direction to guarantee a two-dimensional flow. [Oliver *et al.* (1977)] has shown that if a solid wall has an edge, or any other type of non-uniformity, the contact angle hysteresis is enhanced, reducing the wetting line mobility. Therefore, if the coating die surface has an edge, the contact line may preferentially locate along it: It is common practice in the coating industry to use edges or corners on the coating applicators to "pin" a wetting line.

In principal, the contact line remains on the edge for a range of contact angles θ given by the Gibbs inequality condition, [Gibbs (1906)]:

$$\theta_R < \theta < \theta_A + 180^o - \gamma; \tag{1}$$

where θ, the contact angle, is measured through the liquid phase. The receding contact angle θ_R is the smallest angle achievable before the wetting line begins to move in the direction of the liquid phase. The advancing contact angle θ_A is the largest angle before the wetting line begins to move in the direction of the air phase. γ is the solid edge angle, as show in Fig. 3. The sharper this angle, the greater the hysteresis and the smaller is the wetting-line mobility. This is also a simplified view of the problem, because corners are not mathematical and contact lines do not actually pin. As stated by [Oliver *et al.* (1977)] "...is probable more realistic considerer an edge as a continuous surface without singularities; *i.e.*, it is rounded with $R \neq 0$, so that the contact angle measured to the tangent of the surface (at the submicroscopic level) presumably could remain constant, provided of course that the solid surface is isotropic and energetically homogeneous...".

Corners in coating dies have a specified radius of curvature. The lower limit of its value is set by limitations on the machining process. In this work, the effect of the radius of curvature of the corner between the downstream die lip and die shoulder on the position of the contact line and on the critical conditions at the onset of the low-flow limit is examined by solving the Newtonian flow in the downstream part of the coating bead, as shown in Fig. 1. The contact angle is treated as a specified equilibrium value and the static contact line position is free to move along the surface of the die lip, radius corner and die shoulder. The system of differential equations and boundary conditions was solved by the Galerkin / finite element method. At each operating condition (liquid properties as well as coating gap and web speed), a sequence of states was found by Newton's iterations initialized by first-order, pseudo-arc-length continuation, *i.e.* a solution path in the parameter space was constructed as the flow rate to the die falls.

2. Mathematical Formulation

The flow in the coating bead was described by the two-dimensional, steady state mass and momentum conservation equations for Newtonian liquid.

[Carvalho and Kheshgi (2000)] and [Romero *et al.* (2004)] have shown that at low capillary and Reynolds numbers the flow upstream of the feed slot does not affect the critical operating conditions at the onset of the low-flow limit. Because the analysis presented here focuses on the effect of the radius of curvature of the edge of the downstream slot die at low capillary number and vanishing Reynolds number, the flow domain in which the governing equations are solved is truncated to the region adjacent to the downstream free surface.

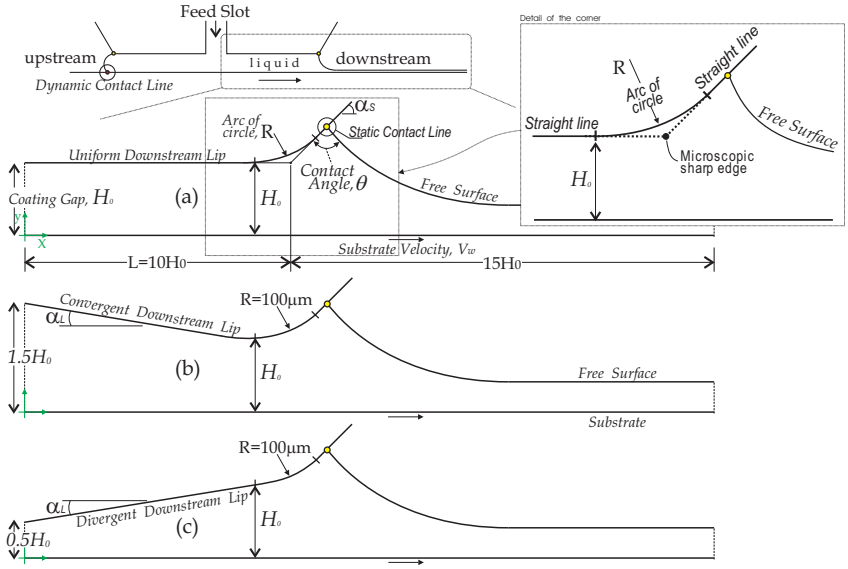

Figure 4. Detail of the downstream slot die showing the three gap configurations used in this work: (a) Uniform ($\alpha_L = 0^o$), (b) Convergent ($\alpha_L = +2.86^o$) and (c) Divergent ($\alpha_L = -2.86^o$). A zoom close to the rounder corner is also shown in the top right side of the figure.

The geometry of the die surface consisted of two straight lines, that represent the die lip and the die shoulder surfaces, connected by an arc of circle, as sketched in Fig. 4. Three different radius of curvature of the corner were analyzed: $R = 200\mu m; R = 100\mu m$ and $R = 50\mu m$. The inclination of the die shoulder with respect to the web was fixed at $\alpha_S = 45^o$. Three different angles between the die lip and the substrate were examined, *e.g.*, $\alpha_L = \pm 2.86^0$ and $\alpha_L = 0^o$, that corresponded to a convergent, divergent and parallel flow channel under the die lip. In all the die configurations, H_0 is the distance of the die lip to the moving web at the intersection of the straight line that represents the die lip with the arc of circle that represents the rounded corner, as indicated in Fig. 4. The obligatory synthetic inflow boundary was a plane placed at $10H_0$ upstream of the point where the two straight lines that represent the die lip and shoulder meet. The similarly obligatory outflow plane was placed $15H_0$ downstream of that same point. Tests confirmed that shifting these planes further upstream and downstream had negligible effect on the results. The ratio of the downstream die lip length (L) to the coating gap in some industrial applications is in the same order of magnitude as the one used here, *i.e.* $L/H_0 \approx 10$.

The velocity $\mathbf{v}$ and pressure p fields of 2D Stokes flow are governed by the continuity and Stokes equations for incompressible Newtonian liquid:

$$\nabla \cdot \mathbf{v} = 0, \qquad -\nabla p + \mu \nabla^2 \mathbf{v} = 0. \tag{2}$$

Where μ is the liquid viscosity.

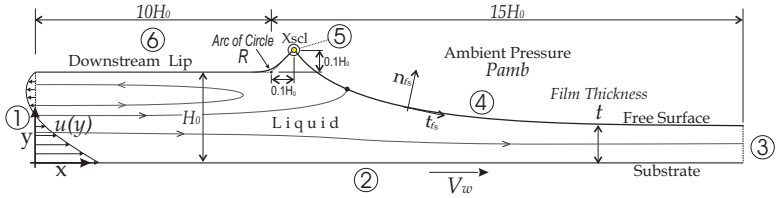

Figure 5. Sketch of flow domain with the boundary conditions.

The boundaries of the flow domain are labeled in Fig. 5 and the correspondent boundary conditions are:

1. *Inflow: Fully developed parallel rectilinear flow, Couette-Poiseuille velocity profile —*

$$u = \frac{6V_w t}{H_0}\left[\left(-1+\frac{1}{2}\frac{H_0}{t}\right)\left(\frac{y}{H_0}\right)^2 + \left(-1+\frac{2}{3}\frac{H_0}{t}\right)\left(\frac{y}{H_0}\right) + \frac{1}{6}\frac{H_0}{t}\right], \qquad v = 0, \tag{3}$$

V_w is the substrate velocity and t is the coating thickness, an input parameter.

2. *Moving substrate: No-slip, no-penetration —*

$$u = V_w, \quad v = 0. \tag{4}$$

3. *Outflow: Fully developed flow —*

$$\mathbf{n} \cdot \nabla \mathbf{v} = 0, \tag{5}$$

$\mathbf{n} \cdot \nabla$ is the directional derivative parallel to the substrate.

4. *Free surface: Force balance and kinematic condition —*

$$\mathbf{n}_{fs} \cdot \mathbf{T} = \sigma \frac{d\mathbf{t}_{fs}}{ds} - \mathbf{n}_{fs} p_{amb}, \qquad \mathbf{n}_{fs} \cdot \mathbf{v} = 0, \tag{6}$$

$\mathbf{t}_{fs}$ and $\mathbf{n}_{fs}$ are the local unit tangent and unit normal to the free surface, $\mathbf{T}$ is the liquid stress tensor ($\mathbf{T} \equiv -p\mathbf{I} + \mu[\nabla \mathbf{v} + \nabla \mathbf{v}^T]$ for Newtonian liquid), σ is the liquid surface tension and p_{amb} is the ambient pressure.

5. *Static contact line: The contact line is free to move with a prescribed contact angle —*

$$\mathbf{n}_w \cdot \mathbf{n}_{fs} = cos(\theta), \tag{7}$$

θ is the angle between the free surface unit normal vector $\mathbf{n}_{fs}$ and the die surface unit normal vector $\mathbf{n}_w$. Two values of the contact angle were considered: $\theta = 90^0$ and $\theta = 45^0$.

6. *Die land: No-slip, no-penetration —*

$$\mathbf{v} = \mathbf{0}. \tag{8}$$

The important dimensionless parameters are: (i) Capillary number $Ca \equiv \frac{\mu V_w}{\sigma}$, which measures the ratio of viscous to capillary forces, (ii) Gap-to-thickness ratio $h \equiv \frac{H_0}{t}$.

3. Solution Method

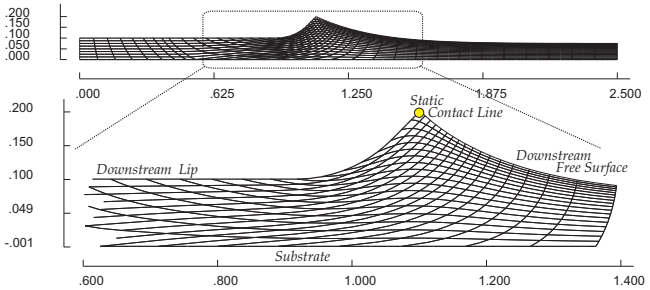

Figure 6. Detail of the mesh used in this work (*Mesh 2* with 568 elements) near the free surface for the uniform slot die configuration with $R = 200\mu m$.

Because of the free surface, the flow domain is unknown *a priori*. Capillarity is comparable to viscous forces in coating flows; fully coupled solution methods (where the position of the interface and the flow solution are computed simultaneously) are superior to fixed-point iterative method where the domain shape and the flow are computed alternatively. Fully coupled methods rely on mapping the unknown physical domain Ω into a known reference domain Ω_0 by means of a bijective transformation $\mathbf{x} = \mathbf{x}(\boldsymbol{\xi})$, where $\mathbf{x}$ and $\boldsymbol{\xi}$ denote position in the physical and reference domain, respectively. The mapping used here was the one described by [De Santos (1991)] and represented in Fig. **??**. The inverse of the mapping –$\boldsymbol{\xi} = \boldsymbol{\xi}(\mathbf{x})$– is governed by a pair of elliptic differential equations identical to those encountered in diffusional transport with variable diffusion coefficients. The coordinates potentials ξ and η of the reference domain satisfy:

$$\nabla \cdot (D_\xi \nabla \xi) = 0, \qquad \nabla \cdot (D_\eta \nabla \eta) = 0, \tag{9}$$

D_ξ and D_η are diffusion-like coefficients used to control gradients in coordinate potentials, and thereby the spacing between curves of constant ξ on the one hand and of constant η on the other that make up the sides of the elements that

were employed; they were quadrilateral elements. Boundary conditions were needed in order to solve the second-order partial differential equations (9). The solid walls and synthetic inlet and outlet planes were described by functions of the coordinates and along them stretching functions were used to distribute the terminii of the coordinate curves selected to serve as element sides. The free boundary (gas-liquid interface) required imposing the kinematic condition, *viz.* eq. (6)(b). The discrete version of the mapping equations is generally referred to as mesh generation equations.

The set of differential equations that describe the conservation of mass and momentum eq. (2) and define the mapping between the physical and reference domain eq. (9), together with the appropriate boundary conditions are all solved on the reference domain Ω_0 by the Galerkin / Finite Element Method.

The position and velocity fields are represented by Lagrangian biquadratic basis functions and the pressure field by linear discontinuous basis functions. The mesh generation equations and the momentum equation are weighted with Lagrangian biquadratic basis functions and the continuity equation with linear discontinuous.

The set of nonlinear algebraic equations that arises from applying the method of weighted residuals and the variables representation in terms of basis functions is solved by Newton's method with analytical Jacobian and first order arclength continuation, and a bordering algorithm ([Bolstad and Keller (1986)]). The tolerance of the L2-norm of the residual vector and the last Newton update for each solution was set to 10^{-6}.

The results presented in the next section are computed with *Mesh 2* showed in Fig. 6.

4. Results

Theoretical predictions are presented at different capillary numbers. The operating conditions at the low-flow limit were determined theoretically by following a solution path constructed at a fixed capillary number (e.g. fixed substrate velocity, liquid viscosity and surface tension) by lowering the flow rate, and consequently the thickness of the coated liquid layer. The local contact angle is treated as a specified equilibrium value and the static contact line position is free to move along the surface of the die.

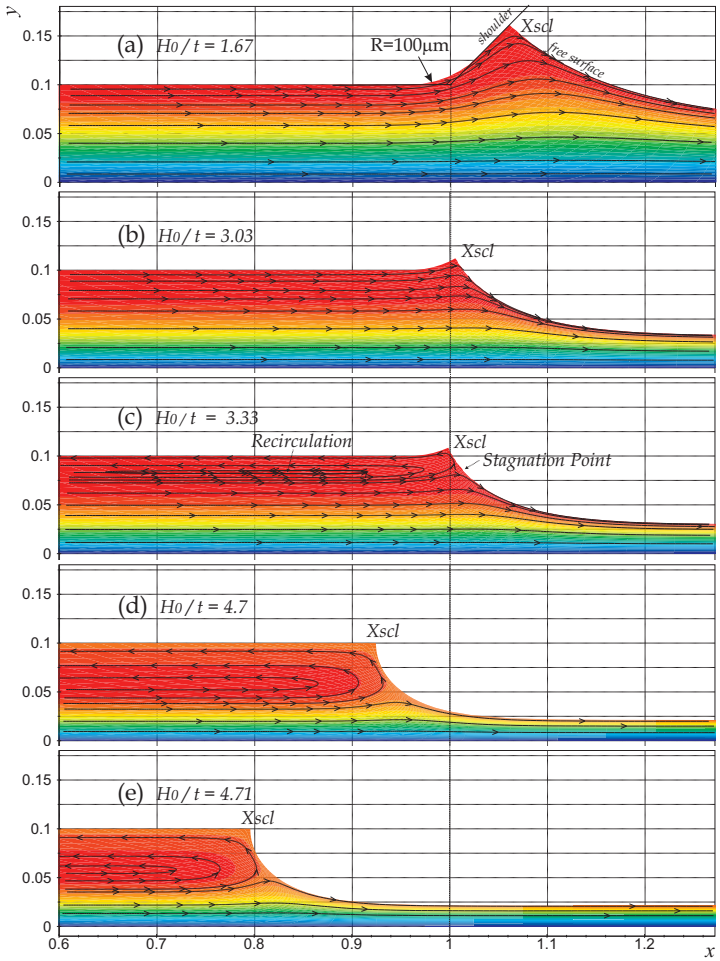

Figure 7. Evolution of the streamlines as the flow rate, *i.e.* film thickness, falls. Uniform slot coating gap with corner radius $R = 100\mu m$, prescribed contact angle $\theta = 90^o$ and capillary number $Ca = 0.17$.

The flow field as a function of the coated layer thickness shown in Fig. 7 at capillary number $Ca = 0.17$, $\alpha_L = 0^o$ (die lip parallel to the substrate), radius of curvature of the die corner $R = 100\mu m$ and contact angle $\theta = 90^0$. At large flow rates, the static contact line is located on the die shoulder. As the thickness of the deposited liquid falls, the adverse pressure gradient driven flow under the die lip becomes stronger and the static contact line moves towards the die corner. At $H_0/t \leq 3.33$ a recirculation appears under the die lip as predicted by lubrication theory. At this condition the static contact line is located at the rounded die corner. As the gap-to-thickness ratio increases even further, the recirculation becomes larger and the meniscus moves toward the inlet plane. At large gap-to-thickness ratio, the sensitivity of the static contact line position to the film thickness is very strong, as it is clear from Fig. 7 (d) and (e).

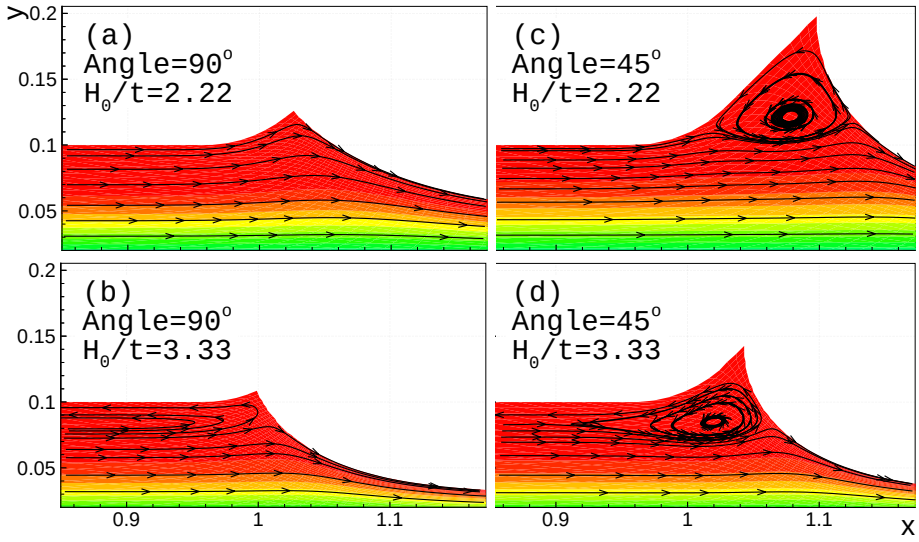

Figure 8. Flow field close the die edge at $R = 100\mu m$ and $\alpha_L = 0^o$. Recirculation under the die shoulder appears when the static contact angle ("Angle" in the caption) is $\theta = 45^o$. Comparisons are for two different gap-to-thickness ratios, *i.e.* $H_0/t = 2.22$ and $H_0/t = 3.33$, contact angles $\theta = 90^o$ and $\theta = 45^o$, and capillary number $Ca = 0.17$.

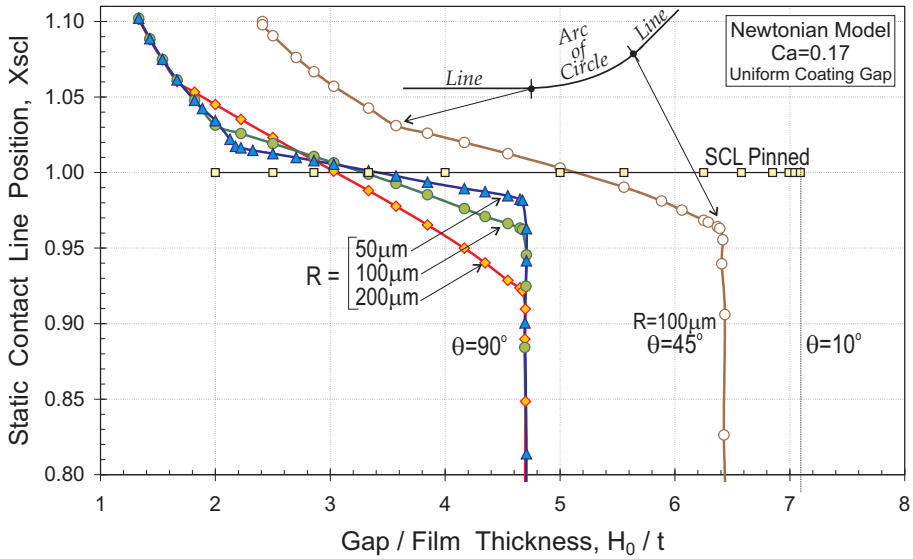

Figure 9. Static contact line position $Xscl$ at different flow rates and radius of curvature ($R = 50\mu m$, $R = 100\mu m$ and $R = 200\mu m$) of the die corner in a uniform slot coating gap with $H_0 = 100\mu m$. The free surface meet the solid wall at $\theta = 90^o$ and $\theta = 45^o$, and is free to slide along it. Newtonian liquid with $Ca = 0.17$

Figure 8 shows the effect of the contact angle on the flow field at $Ca = 0.17$ in a parallel coating gap configuration with a corner radius of curvature $R = 100\mu m$. At contact angle $\theta = 45^o$ the meniscus curvature is more pronounced, leading to a higher pressure jump across the liquid-air interface. At high flow rates, the static contact line moves away

from the die edge, and the length of the die shoulder that is wet by the liquid rises. In this case there is a large recirculation under the die shoulder. The onset of the recirculation under the die lip is virtually independent of the contact angle. At the lower contact angle, the recirculation under the die shoulder merges with the one under the die lip, as shown in Fig. 8 (d).

The liquid trapped in the vortex has very high residence time. In industrial applications solvents may rapidly evaporate leading to deposition of solids on the coating die, making the static contact line not straight and rising the possibility of nonuniformities in the coated layer. Therefore, recirculations under the die shoulder should be avoid in industrial applications. Experimental evidences of this vortex were presented by [Sartor (1990)].

Figure 9 shows the contact line position X_{scl} as the flow rate falls, *i.e.* as the gap over film thickness ratio rises, at different corner radius of curvature R and prescribed contact angles θ. The predictions were obtained at $Ca = 0.17$ in a parallel flow channel ($\alpha_L = 0^o$). The position $X_{scl} = 1$ corresponds to the sharp corner position, *i.e.* the intersection of the straight lines that define the die shoulder and die land. When the contact line is taken to be pinned at the sharp die corner and the contact angle varies with the flow parameters, as done in the model presented by [Carvalho and Kheshgi (2000)] and [Romero *et al.* (2004)], $\theta = 10^o$ is obtained at $H_0/t \approx 7.1$. This was taken to be the critical condition at the onset of the low-flow limit. In the model presented here, the static contact line is free to move along the die surface. At low gap-to-thickness ratio the contact line is located on the die shoulder ($X_{scl} > 1$). The meniscus moves upstream as the flow rate falls (gap-to-thickness ratio rises), moving from the die shoulder to the rounded corner and then to the die land. The position of the contact line as a function of the coated layer thickness is independent of the radius of curvature of the die when it is located over the die shoulder and the die land. On the other hand, the sensitivity of the contact line position to the flow rate is a strong function of the edge curvature when the contact line is located on the rounded corner. At large radius of curvature, *e.g.* $R = 200\mu m$, there is a large variation of the position X_{scl} as the gap-to-thickness ratio varies from $1.7 \leq H_0/t \leq 4.7$. At sharper edge, $R = 50\mu m$, the sensitivity of the position of the contact line to the flow rate is weak, indicating a "pinning" effect.

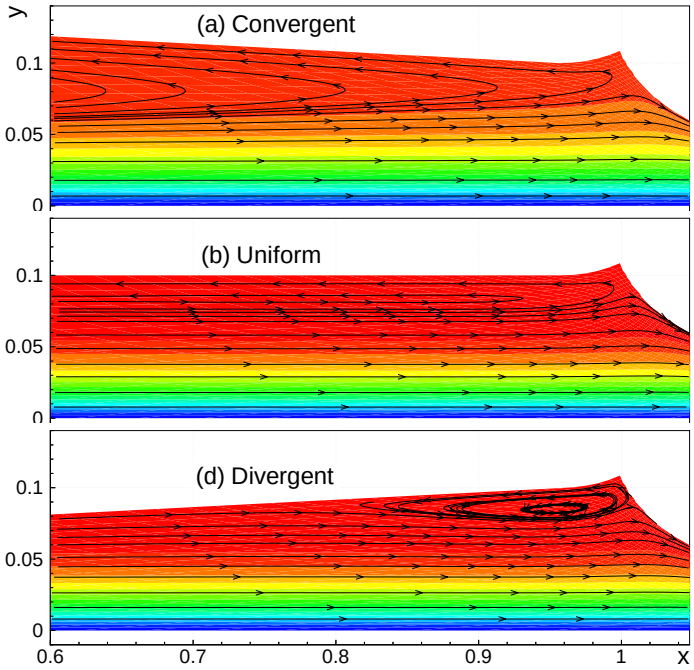

Figure 10. Influence of the angle of the die lip in the flow field. Comparisons are for $H_0/t = 3.33$, $X_{scl} = 1$, $R = 100\mu m$, prescribed contact angle $\theta = 90^o$ and capillary number $Ca = 0.17$.

A turning point in the solution path was not found, but a maximum gap-to-thickness ratio of approximately $H_0/t \approx 4.7$ could be asymptotically determined. The radius of curvature of the die corner does not affect this critical value.

The effect of the static contact angle on the low-flow limit (maximum gap-to-thickness ratio) is also present in Fig. 9. A solution path at $R = 100\mu m$ and $\theta = 45^o$ is also shown in the plot. The sensitivity of the contact line position to the flow rate is not strongly affected by the prescribed contact angle, but the contact angle has a strong effect on the onset of the low-flow limit. The critical condition at $\theta = 45^o$ is $H_0/t \approx 6.4$.

The flow field as a function of the angle of the die lip worth the substrate is shown in Fig. 10 at $H_0/t \approx 3.33$. and $\theta = 90^o$. At this condition, the contact line is located on the rounded corner. Because $H_0/t > 3$, a recirculation under the die lip is presented in all the three configurations. In the divergent flow channel the recirculation is limited to small region under the die land close the free surface.

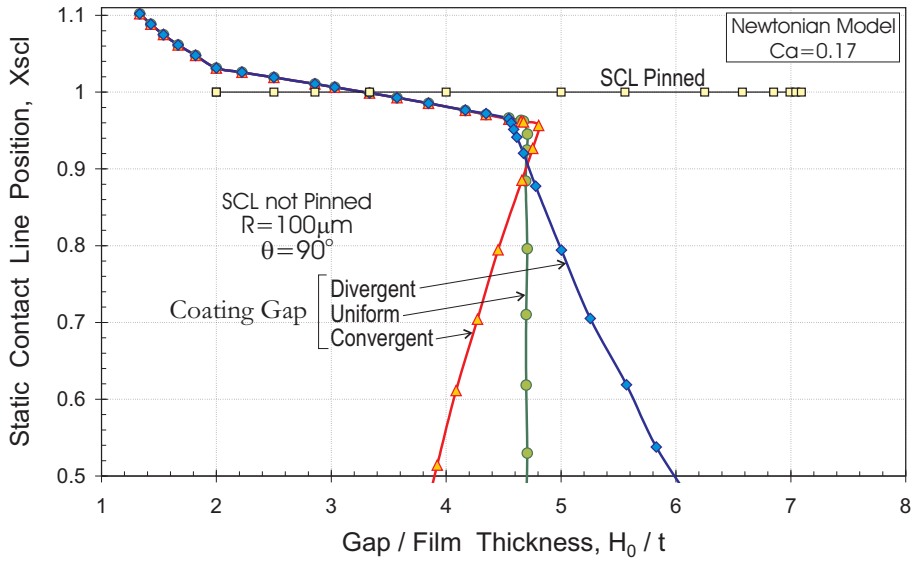

Figure 11. Static contact line position $Xscl$ for coating dies with different die lip angle: $\alpha = -2.86^o$ (divergent), $\alpha = 0^o$ (uniform) and $\alpha = +2.86^o$ (convergent) and same radius of curvature $R = 100\mu m$. Newtonian liquid with $Ca = 0.17$.

Figure 11 presents the variation of the contact line position with flow rate at $R = 100\mu m$, $\theta = 90^o$ and $\alpha_L = 0^o$ (parallel), $\alpha_L = -2.86^o$ (divergent) and $\alpha_L = 2.86^o$ (convergent). The coating gap configuration does not affect the contact line position, while it is located along the die shoulder or the rounded corner, but has a strong effect on the position of the meniscus when the contact line is located on the die lip. The geometry with a convergent channel ($\alpha_L > 0^o$) presents clearly a turning point in the solution path at $H_0/t \approx 4.8$. Two dimensional solutions cannot be computed beyond this value of gap-to-thickness ratio. There is a small increase in the maximal gap-to-thickness ratio when compared to a parallel die lip configuration. This occurs because the edge angle of the die is smaller in this case, enhancing the pinning effect, as described in Fig. 3 and eq. (1).

The die configuration with divergent flow channel ($\alpha_L < 0^o$) has no limit on the gap-to-thickness ratio, the sensitivity of the contact line position to the film thickness is a function of the inclination angle of the die land. As mentioned before, when the die lip is parallel to the web, there is no clear turning point, but a limit of the gap-to-thickness ratio can be determined asymptotically, as a degenerated turning point.

5. References

Beguin, A. L., 1954, "Method of Coating Strip Material", *U.S.Pat.2,681,294*.

Gibbs, J. W., 1906, "Scientific Papers", **1**, p. 326, Dover Reprint, Dover, New York, 1961

Oliver, J. F., Huh, C. and Mason, S. G., 1977, "Resistance to Spreading of Liquids by Sharp Edges". *Journal of Colloid and Interface Science*, **59**, 3, 568-581.

Bolstad, J. H. and Keller, H. B., 1986, "A multigrid continuation method for elliptic problems with folds". *SIAM Journal of Science Stat. Comput*, **7**, 1081-1104.

Carvalho, M. S. and Khesghi, H. S., 2000, "Low-flow limit in slot coating: Theory and Experiments", *AIChE Journal*, **46**, 1907-1917.

De Santos, J. M., 1991, "Two-phase cocurrent downflow through constricted passages". *PhD Thesis, University of Minnesota*, MN.

Romero, O.J., Suszynski, W.J., Scriven, L.E. and Carvalho, M.S., 2004, "Low-flow limit in slot coating of dilute solutions of high moleculer weight polymer", *Journal of Non Newtonian Fluid Mechanics*, **118**, 137-156.

Romero, O.J., Scriven, L.E. and Carvalho, M.S., 2005, "Slot Coating of Mildly Viscoelastic Liquids", **Submited to** *Journal of Non Newtonian Fluid Mechanics*.

Sartor, L., 1990, "Slot Coating: Fluid Mechanics and Die Design", *Ph.D Thesis, University of Minnesota*.

6. Responsibility notice

The author(s) is (are) the only responsible for the printed material included in this paper